

UNDERSTANDING THE IMPACT OF OPERATIONAL VARIABLES ON ELECTRIC AIRCRAFT BATTERY PERFORMANCE VIA REAL-FLIGHT DATA ANALYSIS

Yeongseok Cho[1], Jaewon Lee[1], Yeseo Kim[1], Chanyoung Jung[2], Seokjun Kang[2] & Junghyun Kim[1]

[1]Department of Aerospace Systems Engineering, Sejong University, Seoul, Republic of Korea
[2]TOFF Mobility, Seoul, Republic of Korea

Abstract

Limited onboard battery energy remains a primary operational constraint for electric aircraft. Battery energy consumption is affected by a variety of operational variables such as mission profile, aircraft weight, and thermal operating conditions. Understanding the impact of these variables under real-flight conditions is essential for improving operational efficiency and supporting energy-aware flight planning. This research proposes a scenario-based operational analysis framework using high-resolution real-flight data collected from a Pipistrel Velis Electro operated by TOFF Mobility. Sensitivity analysis is conducted to identify key operational variables that significantly affect battery current demand and cumulative energy consumption. Comparable operational scenarios are formulated by considering variations in climb profile, aircraft weight condition, and thermal operating condition, and their effects on battery energy consumption are evaluated through phase-wise comparisons and performance metrics. The results show that variations in operational factors lead to measurable differences in battery performance and energy use. The findings highlight the importance of real-flight-data-based operational analysis for understanding electric aircraft energy behavior and provide practical insight for energy-aware operational planning in electric aircraft operations.

Keywords: Electric aircraft, Battery performance optimization, Scenario-based flight test, Real-flight data analysis, Step climb

1. Introduction

Electric propulsion technologies are progressing toward practical deployment in short-range air transportation and Advanced Air Mobility (AAM) applications [1, 2]. Large-scale electrified aviation initiatives, including the National Aeronautics and Space Administration (NASA) Electrified Aircraft Propulsion (EAP) program, are actively being pursued [3, 4], and electric aircraft are increasingly considered important components of future low-emission regional air mobility systems [5]. Despite these developments, the operational capability of electric aircraft remains constrained by the limited energy density of current battery systems. Compared with conventional aviation fuels, lithium-ion batteries provide substantially lower onboard energy storage capability [6, 7], requiring increased battery mass to secure sufficient flight endurance. Electric aircraft operations therefore involve trade-offs among onboard energy, aircraft weight, aerodynamic efficiency, propulsion performance, and battery operating conditions, making efficient battery energy management a critical requirement for practical electric aviation.

Battery energy consumption in electric aircraft is affected by a variety of operational variables, including mission profile, aircraft weight, climb strategy, power demand, and thermal operating conditions. Unlike conventional fuel-based aircraft, electric aircraft maintain nearly constant aircraft mass during flight while exhibiting strong sensitivity to electrical loading and battery thermal behavior [8, 9]. In practical flight operations, battery performance is influenced not only by instantaneous power

https://doi.org/10.71945/icas2026_0521

demand but also by cumulative thermal and electrical loading throughout the mission. High-power phases, such as takeoff and climb, can affect subsequent flight characteristics through accumulated battery loading and temperature-dependent behavior. As a result, even flights with similar mission structures may show different battery current demand and cumulative energy consumption depending on operational and environmental conditions.

Previous studies on electric aircraft energy analysis have mainly focused on analytical modeling [10, 11], simulation-based performance evaluation [12, 13], and operational optimization [14, 15]. These studies have contributed to battery sizing, propulsion system performance assessment, mission-level energy estimation, and energy management strategy development [16, 17]. Simulation and surrogate-modeling approaches have also provided useful insights under controlled operating assumptions [18, 19]. However, many existing studies rely on simplified mission definitions, assumed environmental conditions, or controlled simulation environments, which may not fully capture the operational variability observed during actual flight operations. Data-driven operational analysis using empirical flight data and operational records has also been investigated [20]. However, existing data-driven studies often focus on phase-isolated behavior or simplified operational assumptions [21], limiting their ability to characterize cumulative battery energy behavior across complete flight missions. Real-flight datasets inherently contain multiple simultaneously varying operational and environmental factors, making direct interpretation of individual variable effects difficult [22, 23]. Therefore, there is a need for real-flight-data-based analysis methods that can systematically compare electric aircraft battery responses under comparable operational conditions while accounting for practical variability in flight profiles, aircraft loading, and thermal environments.

To address this need, this research proposes a scenario-based operational analysis framework using high-resolution real-flight data collected from a Pipistrel Velis Electro operated by TOFF Mobility. The proposed framework constructs comparable operational scenarios by considering variations in climb profile, aircraft weight condition, and thermal operating condition. Phase-wise comparisons and performance metrics are then used to evaluate differences in battery current demand and cumulative energy consumption under practical flight environments. In addition, by applying sensitivity analysis to real-flight operational scenarios, this research identifies key operational variables that affect electric aircraft battery performance and provides practical insights for energy-aware operational planning. It is worth mentioning that the primary objective of this research is not to derive universally generalized operational rules, but to identify operational energy behavior tendencies observed under selected real-flight conditions. The remainder of this paper is organized as follows: Section 2 presents the proposed methodology. Section 3 outlines the results and discussion. Section 4 discusses directions for future work and concludes this paper.

2. Proposed Methodology

2.1 Overview

Figure 1 presents the overall workflow of the proposed framework designed to systematically compare battery energy behavior under comparable operational conditions using high-resolution flight data collected from commercial electric aircraft operations. The analysis procedure includes data preprocessing, flight phase segmentation, operational variable analysis, scenario formulation, battery energy estimation, and comparative scenario evaluation. More specifically, flight data is preprocessed and segmented into climb, cruise, and descent phases using a hybrid clustering-based phase identification process. The segmented flight phases provide a consistent basis for phase-wise comparison of battery energy behavior under different operational conditions. Operational variables associated with battery behavior are then analyzed to formulate comparable flight scenarios under different climb profile, aircraft weight, and thermal operating conditions. Battery energy consumption is estimated from the battery power profile through numerical integration. Phase-wise comparisons and energy metrics are subsequently used to evaluate operational differences in battery current demand and cumulative energy consumption across the selected flight scenarios. Details about each component will be discussed in subsequent sections.

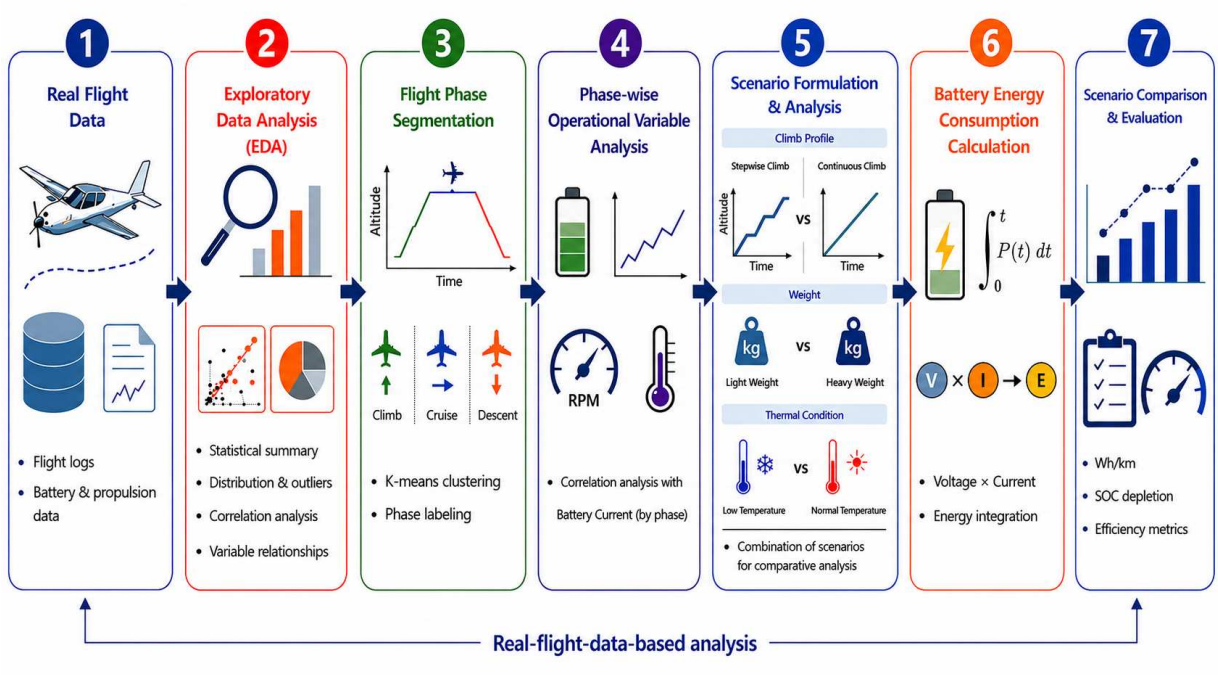


Figure 1 – Overview of the proposed framework

2.2 Exploratory data analysis

The flight datasets used in this research were collected from commercial operations conducted by TOFF Mobility using the Pipistrel Velis Electro, the world's first European Union Aviation Safety Agency type-certified fixed-wing electric aircraft [24]. The aircraft platform used for the real-flight data collection campaign is shown in Figure 2. The datasets consist of synchronized multivariate time-series flight records containing aircraft flight states, battery operating conditions, electric propulsion system parameters, aircraft attitude and position information, and ambient environmental variables recorded throughout flight operations. Battery current, voltage, and temperature measurements were acquired from the onboard Battery Management System (BMS) and Motor Control Unit (MCU).



Figure 2 – Pipistrel Velis Electro aircraft used for real-flight data collection

Exploratory data analysis was first conducted to understand the overall structure, quality, and operational characteristics of the real-flight datasets before performing scenario-based comparisons. The exploratory data analysis involved checking the completeness and consistency of the collected time-series data. Missing values, abnormal spikes, duplicated timestamps, and discontinuities in sensor measurements were examined to ensure that the dataset was suitable for operational analysis. Representative variables included in the real-flight datasets are summarized in Table 1. The datasets include battery-related variables such as state of charge (SoC), battery voltage, battery current, and battery temperature, together with propulsion system parameters including motor torque, motor rota-

tional speed, and electrical power. These variables were used to analyze battery loading characteristics and operational power demand under different flight conditions. Flight dynamics, aircraft attitude and position information, and environmental conditions were also recorded to support phase-wise operational energy analysis and scenario-based flight comparison.

Table 1 – Representative variables included in the real-flight datasets

Category	Representative Variables
Time information	Time stamp, elapsed time
Battery states	SoC, battery voltage, battery current, battery temperature
Electric propulsion system	Motor torque, motor RPM, electrical power
Flight dynamics	Pressure altitude, airspeed, ground speed, vertical speed
Attitude and position	Pitch, roll, yaw, latitude, longitude
Environmental conditions	Outside air temperature, wind speed, wind direction

2.3 Flight phase segmentation

Given that battery load and energy consumption characteristics might vary across different flight phases, the continuous flight logs were segmented into climb, cruise, and descent phases for phase-wise operational analysis. This segmentation was used as a preprocessing step to support consistent comparison of battery energy consumption across different flight scenarios. Initial phase partitioning was performed using the K-means clustering algorithm [25] based on motor torque $T(t)$ and motor rotational speed $\Omega(t)$ as shown in Algorithm 1. At each time step, the feature vector is defined as $\mathbf{x}(t) = [T(t), \Omega(t)]$.

As K-means clustering grouped data based on numerical similarity, an additional physical labeling process was applied to associate each cluster with its corresponding flight phase as shown in Algorithm 2. Each cluster was classified using the mean vertical velocity $\bar{v}_z$ and propulsion load characteristics. The cluster with $\bar{v}_z > 0$ and relatively high motor load was assigned to the climb phase, while the cluster with small $|\bar{v}_z|$ and stable power demand was identified as the cruise phase.

Algorithm 1 K-means-based initial flight phase clustering

Input: Normalized feature vectors $\mathbf{x}(t)$
Initialization: Set $k = 3$; Initialize centroids $\{\mu_1, \mu_2, \mu_3\}$
repeat
  for each time point t **do**
    Assign $\mathbf{x}(t)$ to the nearest centroid $c(t)$
  end for
  for each cluster $j \in \{1,2,3\}$ **do**
    Update centroid μ_j
  end for
until centroids converge
Output: Cluster label $c(t)$

Algorithm 2 Physical flight phase labeling

Input: Cluster labels $c(t)$, torque $T(t)$, RPM $\Omega(t)$, vertical speed $v_z(t)$
for each cluster $j \in \{1,2,3\}$ **do**
  Compute mean vertical speed $\bar{v}_{z,j}$ and propulsion load characteristics
  if $\bar{v}_{z,j} > 0$ and motor load is high **then**
    Label cluster j as **Climb Phase**
  else if $|\bar{v}_{z,j}|$ is small and power demand is stable **then**
    Label cluster j as **Cruise Phase**
  else if $\bar{v}_{z,j} < 0$ and motor load is low **then**
    Label cluster j as **Descent Phase**
  end if
end for
Output: Finalized flight phase labels

A representative result of the proposed phase segmentation procedure is shown in Figure 3. The continuous flight log is separated into climb, cruise, and descent phases corresponding to physically interpretable operating conditions. This segmented structure provides the basis for subsequent scenario-based operational energy analysis.

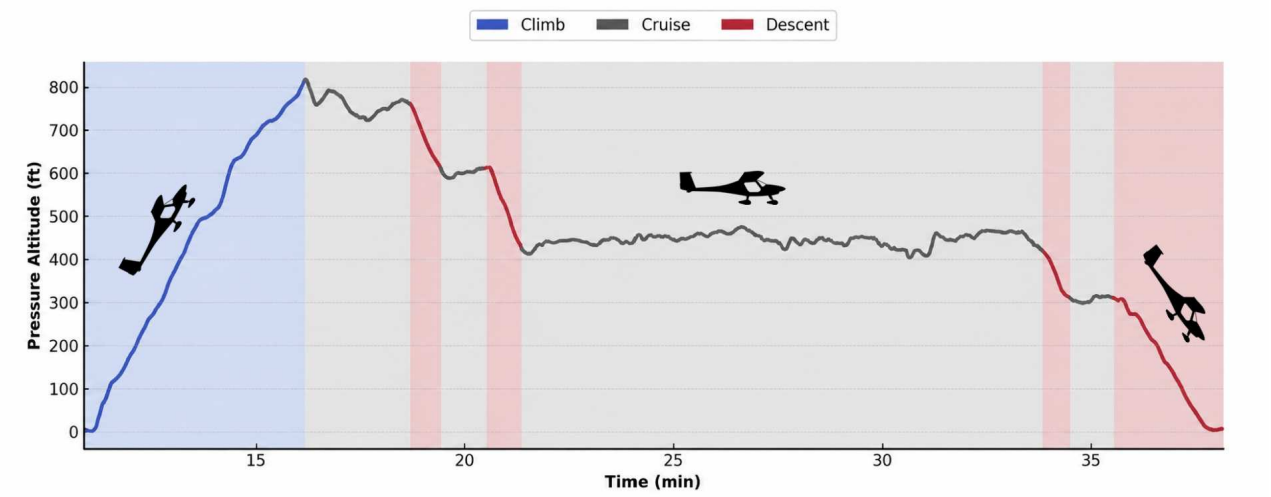


Figure 3 – Results of the flight phase segmentation procedure

2.4 Phase-wise correlation analysis

After flight phase segmentation, a phase-wise correlation analysis was conducted to investigate the relationships between battery current and representative operational variables under different flight conditions. Battery current was selected as the primary response variable as it directly reflected instantaneous propulsion power demand. The analysis was performed separately for climb, cruise, and descent phases to identify phase-dependent operational characteristics that may not be observable from the complete flight dataset.

2.4.1 Climb phase

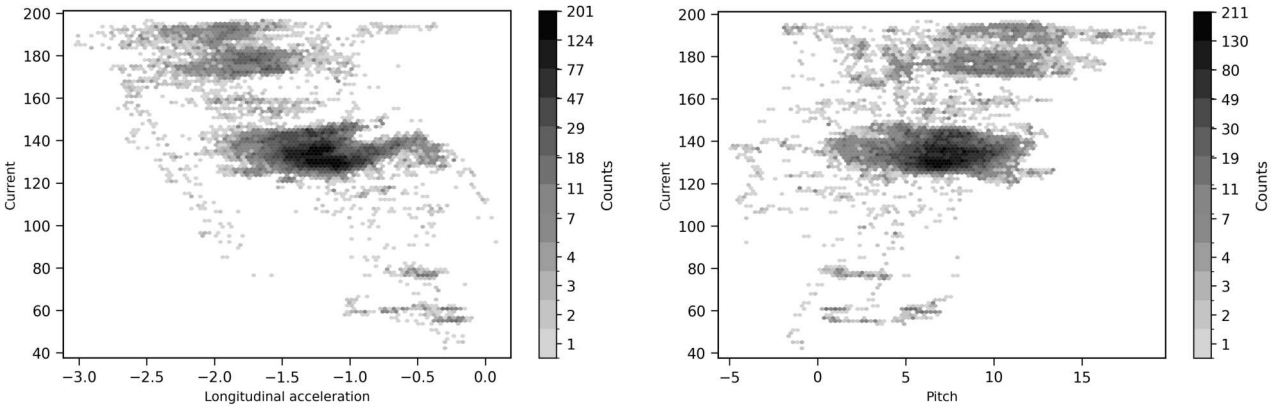
Figure 4 illustrates the correlation results for the climb phase. Among the operational variables, pitch angle exhibited the clearest positive relationship with battery current, indicating that climb-phase battery demand is strongly associated with sustained propulsion loading required for altitude gain. Longitudinal acceleration showed a generally negative relationship with battery current, suggesting that propulsion power during climb is primarily consumed for maintaining climb performance rather than forward acceleration. These tendencies indicate that climb profile is one of the dominant operational factors affecting battery loading during real-flight operations.

2.4.2 Cruise phase

Figure 5 presents the cruise-phase correlation results. Compared with the climb phase, battery current variation during cruise was more closely associated with thrust adjustment and aerodynamic trim maintenance than with altitude-gain demand. Pitch angle maintained a positive relationship with battery current, while longitudinal acceleration remained concentrated within a relatively narrow operating region. These results indicate that cruise-phase battery demand is influenced by continuous propulsion adjustment required to maintain stable flight conditions.

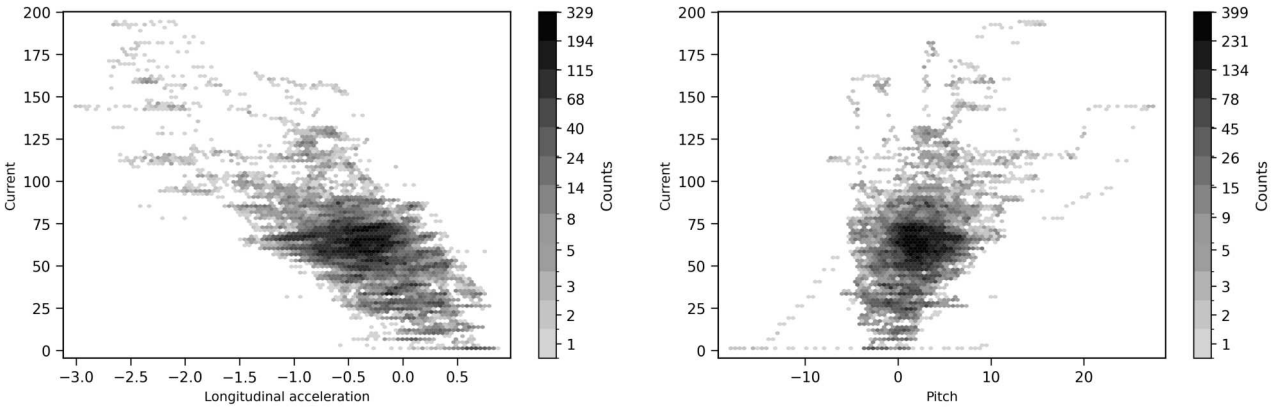
2.4.3 Descent phase

Figure 6 shows the descent-phase correlation results. Compared with climb and cruise operations, battery current during descent remained concentrated within a low-current region, reflecting the relatively low propulsion demand required during descent flight. The relationships between operational variables and battery current were therefore less pronounced than in the climb phase. Compared



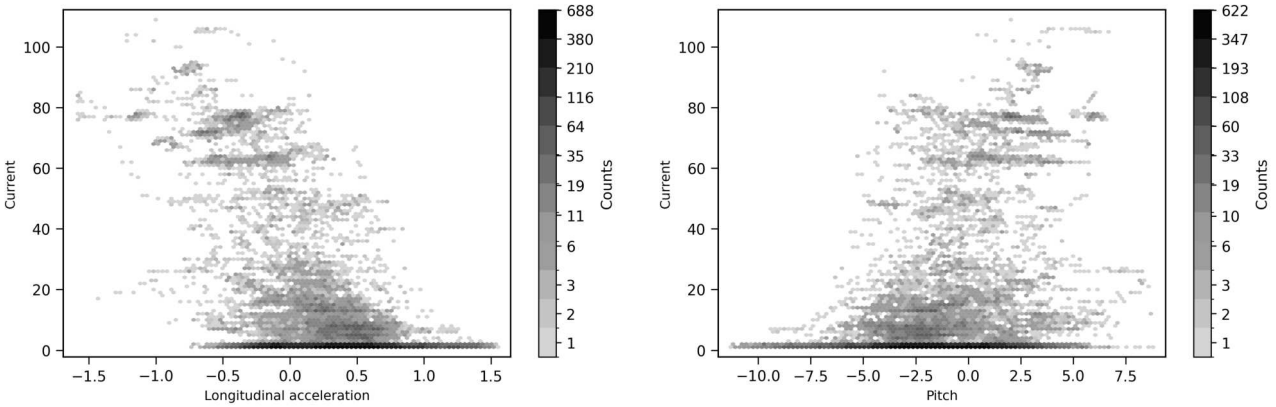
(a) Longitudinal acceleration (b) Pitch angle

Figure 4 – Correlation between battery current and selected operational variables (Climb)



(a) Longitudinal acceleration (b) Pitch angle

Figure 5 – Correlation between battery current and selected operational variables (Cruise)



(a) Longitudinal acceleration (b) Pitch angle

Figure 6 – Correlation between battery current and selected operational variables (Descent)

with climb operations, the descent phase exhibited relatively weak relationships between operational variables and battery current due to the lower propulsion demand observed during descent flight.

Overall, the correlation analysis indicates that battery current behavior is strongly affected by propulsion-loading characteristics associated with different flight phases. Among the operational variables, pitch angle and propulsion-loading characteristics exhibited the clearest relationships with battery current across different operational conditions. These observations provide the basis for the subsequent scenario-based analysis of operational variables.

2.5 Scenario-based flight test design

Scenario-based flight tests were designed to evaluate the influence of operational variables on battery energy consumption under comparable real-flight conditions. As actual flight data contained variations in pilot input, wind condition, and battery thermal history, each scenario was constructed to vary a specific operational variable while maintaining the remaining flight conditions within a comparable operational range. Three operational scenarios were considered in this research: climb profile, aircraft weight, and thermal operating condition.

2.5.1 Climb profile scenario

The climb profile scenario was designed to evaluate the impact of climb trajectory structure on battery energy consumption. Two climb strategies were compared: continuous climb and stepwise climb. Figure 7 shows representative altitude profiles for the two climb strategies. The continuous climb case maintained uninterrupted altitude gain throughout the climb segment, whereas the stepwise climb case included intermediate level-flight segments between climb sections.

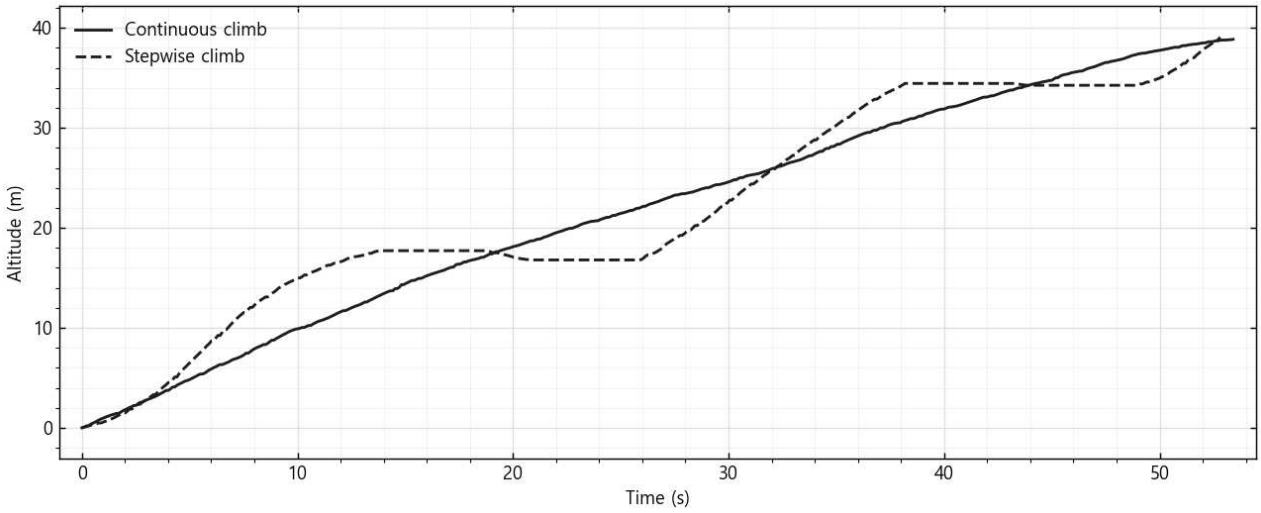


Figure 7 – Representative altitude profiles for the continuous and stepwise climb scenarios

To improve the comparability of the analysis, flight duration, altitude gain, operational airspeed, and other operational conditions were selected within similar ranges between the two real-flight cases. The representative flight conditions used for the climb profile comparison are summarized in Table 2.

Table 2 – Flight conditions of the climb profile scenarios

Item	Continuous climb	Stepwise climb
Climb profile	Continuous climb	Stepwise climb
Aircraft weight	530 kg	530 kg
Outside air temperature	30°C	30°C
Altitude gain	38.9 m	39.1 m
Duration	53.4 s	52.8 s
Mean climb rate	0.73 m/s	0.74 m/s
Mean indicated airspeed	73.3 KIAS	76.1 KIAS

2.5.2 Weight condition scenario

The weight condition scenario was designed to evaluate the influence of aircraft gross weight on battery energy consumption under comparable flight conditions. Two aircraft weight conditions were compared: 530 kg and 603 kg. Figure 8 shows representative altitude profiles for the weight condition scenarios.



Figure 8 – Representative altitude profiles for different aircraft weight conditions

Flight duration, altitude profile, operational airspeed, and initial battery state were selected within comparable operational ranges between the two weight conditions. Phase-wise energy consumption, battery current, power consumption, and total mission energy consumption were then compared between the two aircraft weight conditions. The representative flight conditions used for the weight comparison are summarized in Table 3.

Table 3 – Flight conditions of the weight condition scenarios

Item	530 kg condition	603 kg condition
Aircraft weight	530 kg	603 kg
Mission profile	Repeated climb–descent	Repeated climb–descent
Analysis duration	639.6 s	675.5 s
Altitude range	97.8 m	95.7 m
Mean indicated airspeed	70.1 KIAS	69.3 KIAS
Mean climb power	52.2 kW	53.7 kW

2.5.3 Thermal operating condition scenario

The thermal operating condition scenario was designed to evaluate the impact of thermal operating environment on battery energy consumption under comparable operational conditions. Two thermal operating conditions were compared: low-temperature condition and normal-temperature condition. Figure 9 shows representative altitude profiles for the two thermal operating conditions.

Flight duration, altitude profile, and operational airspeed were selected within comparable operational ranges between the two temperature conditions. The comparison reflects the combined influence of outside air temperature, initial battery temperature, and in-flight thermal response under

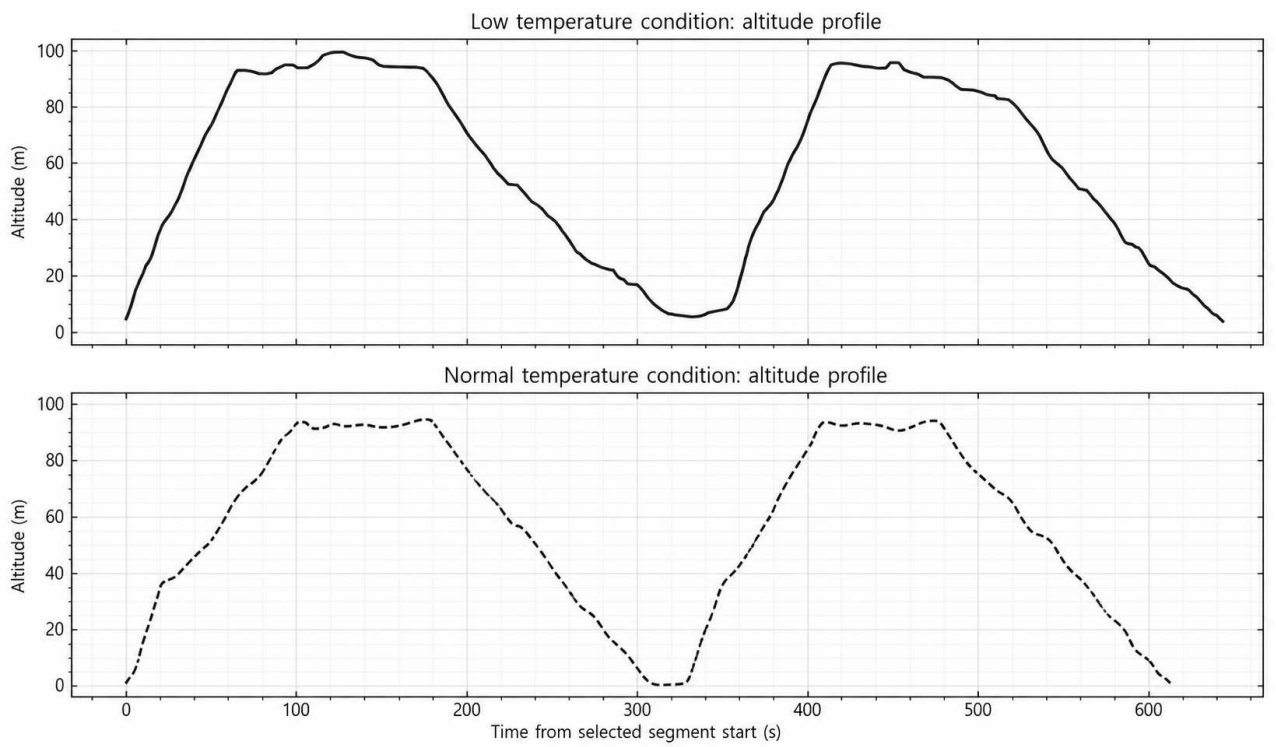


Figure 9 – Representative altitude profiles for the low-temperature and normal-temperature

actual operating conditions. The representative flight conditions used for the thermal operating condition comparison are summarized in Table 4.

Table 4 – Flight conditions of the thermal operating condition scenarios

Item	Low temperature	Normal temperature
Outside air temperature	4.0°C Avg.	23.14°C Avg.
Flight pattern	Repeated climb–descent	Repeated climb–descent
Pressure altitude range	Approximately 1,000 ft	Approximately 1,000 ft
Mission duration	About 10.6–10.9 min	About 10.6–10.9 min
Initial SOC	90%	90%
Initial battery temperature	8°C at takeoff	29°C at takeoff

2.6 Battery energy efficiency analysis

The energy efficiency analysis framework was developed to evaluate battery energy consumption under different operational conditions. Energy consumption was analyzed for both the complete mission and individual flight phases using representative operational metrics. The framework additionally considered comparability between baseline and comparison scenarios before evaluating energy-efficiency differences.

2.6.1 Calculation of battery energy consumption

Battery energy consumption was calculated using the battery voltage and current recorded in the real-flight datasets. Instantaneous battery power was defined as:

$$P(t) = V(t)I(t) \tag{1}$$

where $V(t)$ and $I(t)$ denote battery voltage and current, respectively. Battery energy consumption for each flight segment was obtained by integrating the power profile over time:

$$E = \frac{1}{3600}\int_{t_{\text{start}}}^{t_{\text{end}}} V(t)I(t)\,dt \tag{2}$$

As the flight logs consisted of discrete time-series data, numerical integration was applied as follows:

$$E \approx \frac{1}{3600} \sum_{n=1}^{N-1} V(t_n) I(t_n) \Delta t_n \tag{3}$$

Energy consumption was evaluated for both the complete mission and the climb, cruise, and descent phases. Distance-normalized energy consumption was also calculated to account for differences in actual flight distance between scenarios with the following equation. Here, D_{ground} denotes the traveled ground distance.

$$E_{\text{dist}} = \frac{E}{D_{\text{ground}}} \tag{4}$$

2.6.2 Energy efficiency metrics for scenario comparison

Energy efficiency was evaluated using multiple metrics as shown in Table 5. Total energy consumption was utilized to compare overall battery usage between scenarios, while distance-normalized energy consumption was used to account for differences in actual flight distance. Average battery current and average power were used to interpret propulsion loading during flight operation. Phase-wise energy consumption was additionally evaluated to identify whether the impact of each operational variable was concentrated in a specific flight phase or accumulated throughout the mission.

Table 5 – Energy efficiency metrics for scenario comparison

Metric	Description
Total energy consumption [Wh]	Total battery energy used during flight
Distance-normalized energy consumption [Wh/km]	Battery energy consumption per unit flight distance
Average battery current [A]	Average current load required from the battery
Average power [kW]	Average electrical power demand during flight
Phase-wise energy consumption [Wh]	Energy consumption during different phases (i.e., climb, cruise, and descent)

The relative change in energy consumption between the baseline and comparison scenarios was calculated by the following equation. Here, E_{base} and E_{scenario} denote the energy consumption of the baseline and comparison scenarios, respectively. This metric was used to quantify the impact of each operational variable on battery energy consumption.

$$\Delta E_{\text{rel}} = \frac{E_{\text{scenario}} - E_{\text{base}}}{E_{\text{base}}} \times 100 \tag{5}$$

2.6.3 Assessment of comparability between scenarios

The scenario comparison was based on a baseline-versus-comparison structure. For each scenario, a representative operational variable was intentionally varied while the remaining flight conditions were maintained within comparable operational ranges. The target operational variables considered in this research were climb trajectory structure, aircraft gross weight, and thermal operating condition. To improve comparability between scenarios, flight dynamics variables, propulsion-load variables, environmental conditions, and battery states were reviewed before energy comparison. As these variables had different physical units and numerical ranges, the min–max normalization technique was employed before comparison:

$$X_i'(t) = \frac{X_i(t) - X_{i,\min}}{X_{i,\max} - X_{i,\min}} \tag{6}$$

The normalized variables were used to calculate group-wise differences between the baseline and comparison scenarios using the following equations. Here, D_k denotes the group-wise difference

between the baseline and comparison scenarios and ε_k denotes the allowable threshold for the corresponding variable group.

$$D_k = \frac{1}{|V_k|} \sum_{i \in V_k} \left| \overline{X}'_{i,\text{baseline}} - \overline{X}'_{i,\text{scenario}} \right| \tag{7}$$

$$D_k \leq \varepsilon_k \tag{8}$$

It is important to note that this condition was used as a practical comparability guideline rather than a strict statistical acceptance criterion. The target operational variable was required to remain sufficiently distinguishable between the baseline and comparison scenarios:

$$\Delta X_{\text{target}} = \left| \overline{X}'_{\text{target,baseline}} - \overline{X}'_{\text{target,scenario}} \right| \geq \varepsilon_{\text{target}} \tag{9}$$

where ΔX_{target} denotes the difference in the target operational variable between the two scenarios. It should be noted that scenario comparison was performed only when the major flight-condition differences remained sufficiently limited relative to the target operational variable while the target operational variable itself remained clearly distinguishable between the baseline and comparison scenarios.

3. Results and Discussion

This section presents the scenario-based battery energy consumption results obtained from the real-flight datasets. The analysis focuses on operational energy tendencies observed under different climb profiles, aircraft-weight conditions, and thermal operating conditions. Representative battery current, power consumption, and energy consumption characteristics are comparatively analyzed for each operational scenario. Details will be discussed in subsequent sub-sections.

3.1 Results of the climb profile scenario analysis

Two climb strategies, continuous climb and stepwise climb, were compared under similar flight duration, altitude gain, and operational airspeed conditions. Figure 10 shows the comparison of battery current responses for the two climb strategies. The continuous climb case exhibited relatively sustained current behavior during the climb segment, whereas the stepwise climb case showed repeated current fluctuations associated with intermediate level-flight segments. Temporary reductions in current demand appeared during the level-flight intervals of the stepwise climb profile.

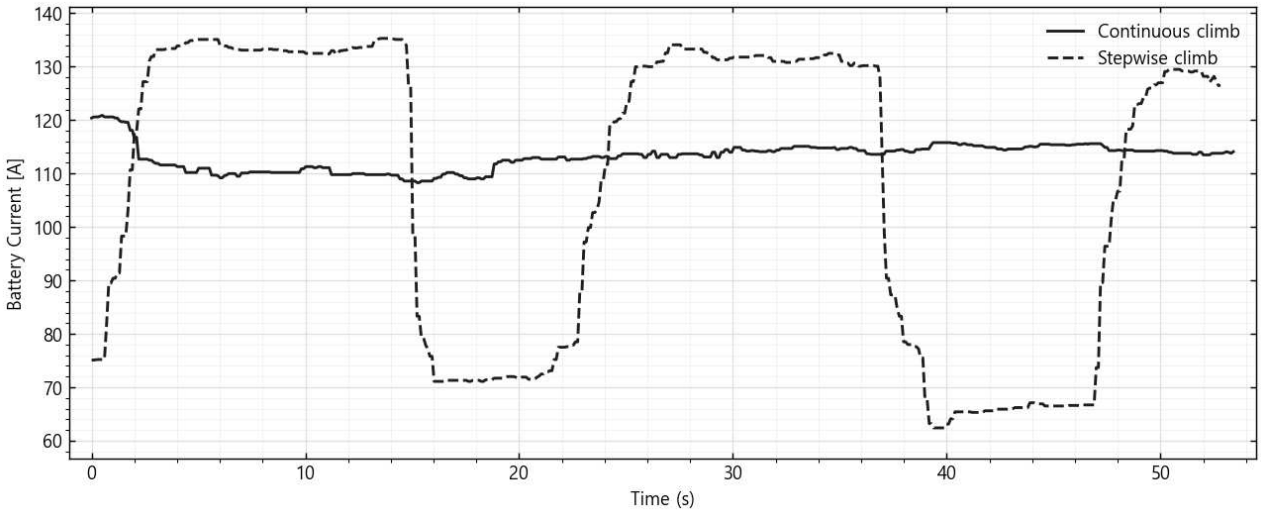


Figure 10 – Continuous climb vs. stepwise climb with respect to battery current

Table 6 summarizes the quantitative energy-consumption results for the climb profile scenario. It seems that the stepwise climb case showed lower climb-phase current, lower power consumption, and lower climb-phase energy consumption compared with the continuous climb case. The average

climb-phase current decreased from 113.16 A to 107.44 A, and climb-phase energy consumption decreased from 612.98 Wh to 568.96 Wh. Distance-normalized and altitude-normalized energy consumption also showed lower values in the stepwise climb condition. Compared with the continuous climb case, the stepwise climb strategy exhibited a 7.18% reduction in climb-phase energy consumption relative to the baseline condition.

Table 6 – Energy consumption results for the climb profile scenario

Item	Continuous climb	Stepwise climb
Average climb-phase current [A]	113.16	107.44
Average climb-phase power [kW]	41.24	38.71
Climb-phase energy consumption [Wh]	612.98	568.96
Distance-normalized energy consumption [Wh/km]	507.86	458.19
Altitude-normalized energy consumption [Wh/m]	15.77	14.55
Energy variation relative to baseline [%]	Baseline	-7.18

The observed difference between the two climb strategies implies that climb-profile design can influence battery energy behavior even when the final altitude gain is nearly identical. As both cases were selected under similar climb duration, altitude gain, and operational airspeed conditions, the difference in energy consumption is likely associated with the temporal distribution of propulsion demand rather than the total altitude change itself. The continuous climb case maintained a relatively sustained high-current operating condition, while the stepwise climb case included intermediate level-flight intervals that temporarily reduced battery current demand. For electric aircraft, this reduction in sustained high-current operation can be beneficial because battery-related electrical losses and thermal loading tend to increase under higher current demand. Thus, redistributing the climb load through short level-flight segments may slightly reduce cumulative battery energy consumption during the climb phase. However, given that the magnitude of the observed reduction is relatively small, additional repeated flight tests are required to further validate this tendency.

3.2 Results of the aircraft weight scenario analysis

Two aircraft-weight conditions were compared: 530 kg and 603 kg. Figure 11 compares the cumulative energy consumption under the 530 kg and 603 kg aircraft-weight conditions.

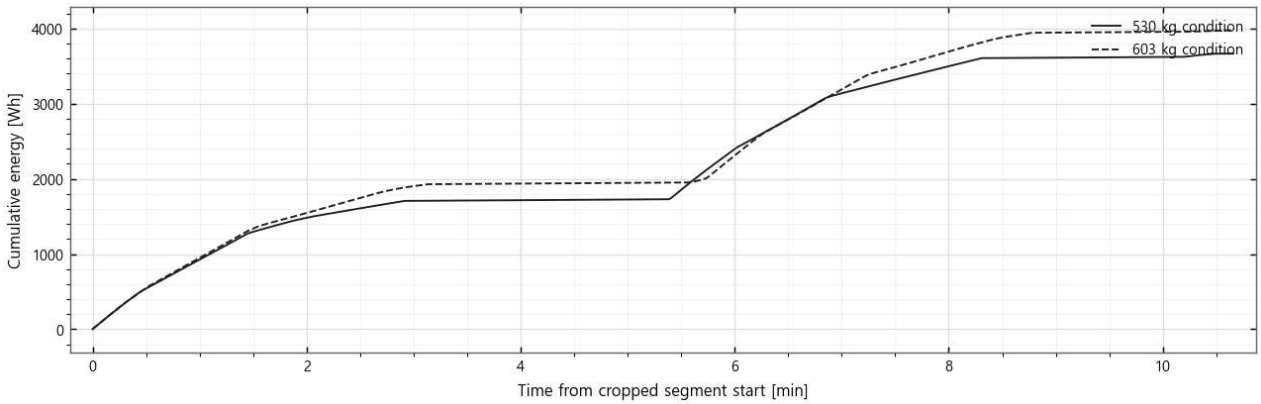


Figure 11 – Comparison of the cumulative energy consumption under 530 kg and 603 kg conditions

It appears that the heavier aircraft condition showed higher energy consumption than the lighter aircraft condition. As can be seen, the 603 kg condition exhibited greater total flight energy consumption compared with the 530 kg condition. Total flight energy consumption increased from 3666.18 Wh to 4021.68 Wh, corresponding to a 9.70% increase relative to the 530 kg baseline condition. The SOC reduction also increased from 18.00% to 19.00%, indicating that the heavier aircraft condition required a larger portion of the available battery capacity.

3.3 Results of the thermal condition scenario analysis

The low-temperature and normal-temperature conditions were compared under comparable operational and altitude-profile conditions. Figure 12 shows the comparison of the battery current responses under the two thermal conditions. The low-temperature condition generally exhibited higher current demand than the normal-temperature condition across the analyzed flight segment.

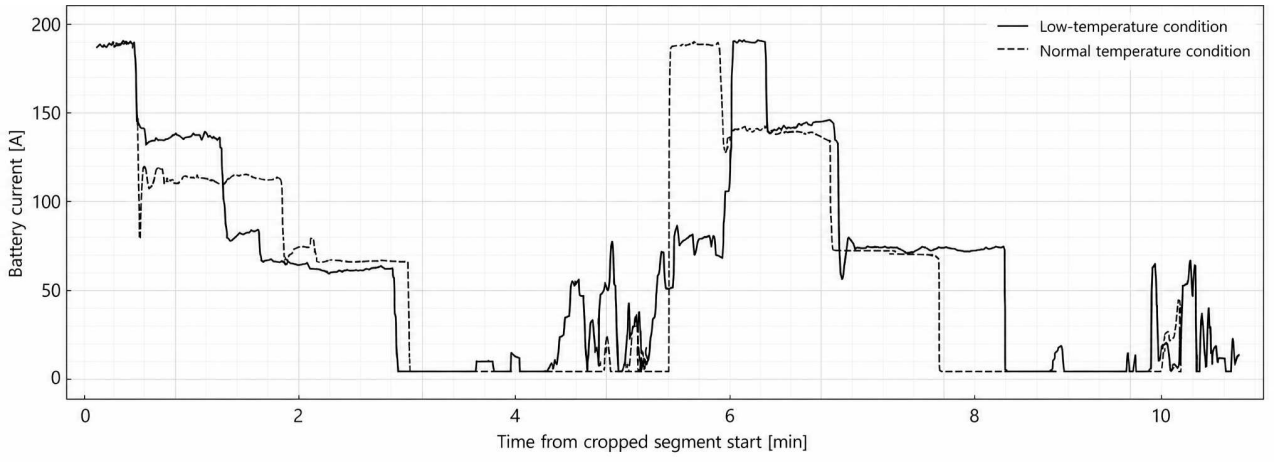


Figure 12 – Low temperature vs. normal temperature with respect to battery current

Figure 13 shows the comparison of the battery voltage responses under the two thermal conditions. The normal-temperature condition maintained a generally higher battery voltage level than the low-temperature condition, indicating a more stable voltage response under warmer operating conditions.

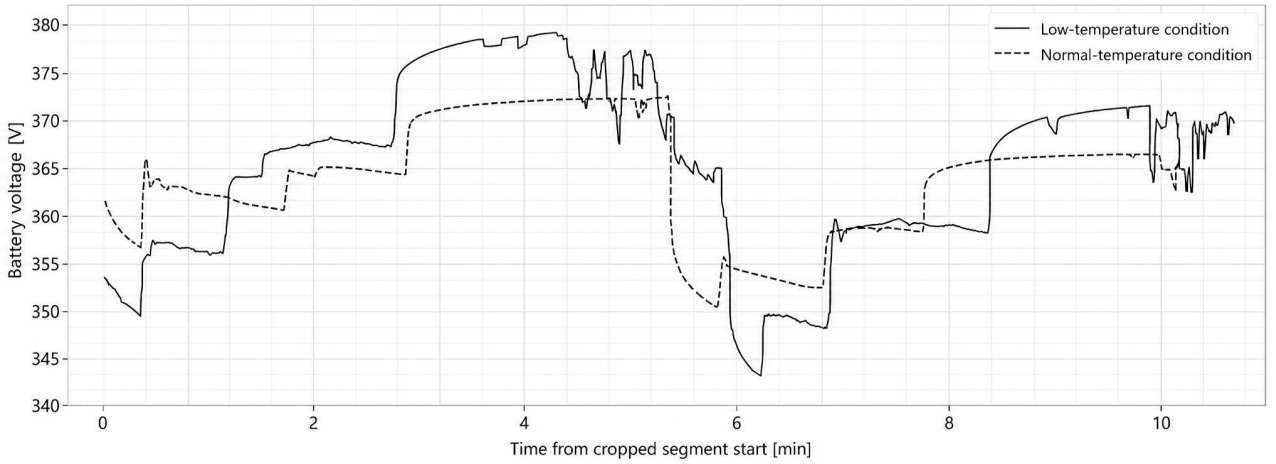


Figure 13 – Low temperature vs. normal temperature with respect to battery voltage

Table 7 – Comparison of flight performance metrics under low- and normal-temperature conditions

Item	Low-temp.	Normal-temp.
Average climb-phase current [A]	148.17	139.06
Average cruise-phase current [A]	56.57	59.78
Average descent-phase current [A]	11.67	2.67
Average climb-phase power [kW]	52.04	49.59
Average cruise-phase power [kW]	20.54	21.55
Average descent-phase power [kW]	4.30	0.98
Average total flight power [kW]	21.08	20.83
Total flight energy consumption [Wh]	3773.25	3558.22
SOC reduction [%]	19.50	17.00
Energy variation relative to low-temp. [%]	Baseline	-5.70

Table 7 summarizes the quantitative comparison of the battery-load and energy-consumption results for the thermal operating condition scenario. As illustrated, the normal-temperature condition exhibited lower climb-phase current, lower climb-phase power, lower total flight energy consumption, and lower SOC reduction compared with the low-temperature condition. Total flight energy consumption decreased from 3773.25 Wh to 3558.22 Wh, corresponding to a 5.70% reduction relative to the low-temperature baseline condition. The average climb-phase current decreased from 148.17 A to 139.06 A, while the average climb-phase power decreased from 52.04 kW to 49.59 kW under the normal-temperature condition. The SOC reduction also decreased from 19.50% to 17.00%, indicating that the normal-temperature condition required a smaller portion of the available battery capacity during the analyzed flight operation.

4. Conclusion

This research proposed a scenario-based operational analysis framework to investigate the impact of operational variables on electric aircraft battery performance using high-resolution real-flight data. The analysis was conducted using flight datasets collected from a Pipistrel Velis Electro operated by TOFF Mobility. To support systematic comparison under practical flight conditions, the proposed framework included exploratory data analysis, flight phase segmentation, phase-wise correlation analysis, scenario-based flight test design, and battery energy efficiency analysis. It is important to note that the primary objective of this research was not to derive universally generalized operational rules, but to identify battery energy behavior tendencies observed under selected real-flight conditions.

The results indicate that electric aircraft battery performance is affected by operational variables such as climb profile, aircraft weight, and thermal operating condition. In the climb profile scenario, the stepwise climb case showed lower climb-phase current demand, power consumption, and energy consumption than the continuous climb case under the conditions. This implies that the temporal distribution of propulsion demand during climb can influence battery energy use. In the aircraft weight scenario, the heavier aircraft condition resulted in higher total flight energy consumption. This tendency reflects the additional propulsion requirement associated with increased aircraft weight. In the thermal operating condition scenario, the low-temperature condition showed higher current demand, lower voltage response, and higher total energy consumption than the normal-temperature condition. These results highlight the importance of considering battery thermal operating conditions when interpreting electric aircraft energy behavior.

The main contribution of this research is the development and demonstration of a real-flight-data-based analysis framework for comparing electric aircraft battery responses under comparable operational scenarios. Unlike purely simulation-based studies or direct comparisons of arbitrary flight logs, the proposed framework uses phase-wise comparison, performance metrics, and scenario-based analysis to improve the interpretability of operational battery behavior. The findings show that real-flight datasets can provide practical insights into how operational decisions and environmental conditions affect battery current demand and cumulative energy consumption. However, given that the analysis was conducted using real-flight operational data, several limitations should be acknowledged. For example, although the selected scenarios were formulated to maintain comparable flight conditions, real-flight operations inevitably included uncontrolled variations such as wind condition, pilot input, atmospheric disturbance, speed-tracking difference, and battery thermal history. Thus, the results should be interpreted as operational tendencies observed from practical flight data rather than isolated effects of individual variables under fully controlled experimental conditions.

Future work will focus on extending the proposed framework in two directions. First, additional real-flight datasets and repeated flight tests under more controlled operating conditions will be used to improve statistical reliability and further validate the observed operational tendencies. Second, the real-flight analysis results will be used to support the development of simulation models that can mimic practical electric aircraft battery behavior. Once a reliable baseline simulation model is established, it can be further used for design space exploration, sensitivity analysis, surrogate modeling, battery performance optimization, and what-if scenario analysis. These future efforts are expected to support battery-aware operational planning and performance optimization for electric aircraft under realistic flight environments.

5. Acknowledgment

This research was supported by TOFF Mobility and the MSIT (Ministry of Science and ICT), Korea, under the ITRC (Information Technology Research Center) support program (IITP-2026-RS-2024-00437494) supervised by the IITP(Institute for Information & Communications Technology Planning & Evaluation).

6. Corresponding Author Email Address

For more information, please reach out to the corresponding author at: junghyun.kim@sejong.ac.kr

7. Copyright Statement

The authors confirm that they, and/or their company or organization, hold copyright on all of the original material included in this paper. The authors also confirm that they have obtained permission, from the copyright holder of any third party material included in this paper, to publish it as part of their paper. The authors confirm that they give permission, or have obtained permission from the copyright holder of this paper, for the publication and distribution of this paper as part of the ICAS proceedings or as individual off-prints from the proceedings.

References

[1] Bright Appiah Adu-Gyamfi and Clara Good. Electric aviation: A review of concepts and enabling technologies. *Transportation Engineering*, 9:100134, 2022.

[2] B. von den Hoff, R. Merino Martinez, R. M. Yupa Villanueva, and M. Snellen. Noise emissions and noise annoyance of a single-propeller electric aircraft during flyover. In *Proceedings of the 30th International Congress on Sound and Vibration (ICSV30)*, 2024. Article 558, 8 pp.

[3] Ralph H. Jansen, Cheryl L. Bowman, Amy Jankovsky, Rodger W. Dyson, James L. Felder, and Gerald V. Brown. Overview of nasa electrified aircraft propulsion (eap) research for large subsonic transports. Technical Report NASA/CR-2019-220382, National Aeronautics and Space Administration, September 2019.

[4] International Air Transport Association. Aircraft technology roadmap to 2050. Technical report, International Air Transport Association, 2023.

[5] Boeing Commercial Airplanes. Commercial market outlook 2023–2042. Technical report, The Boeing Company, 2023.

[6] Venkat Viswanathan, Alan H. Epstein, Yet-Ming Chiang, Esther Takeuchi, Marty Bradley, John Langford, and Martin Winter. The challenges and opportunities of battery-powered flight. *Nature*, 601(7894):519–525, 2022.

[7] Md Nasir Uddin and Feng Wang. Sustainable aviation fuels: A review of current techno-economic viability and life cycle impacts. *Energies*, 18(20):5510, 2025.

[8] Tavish Pattanayak and Dimitri N. Mavris. Battery technology for sustainable aviation: A review of current trends and future prospects. *Applied Energy*, 397:126356, 2025.

[9] Feifan Yu, Jiajie Chen, Panao Gao, Yu Kong, Xiaokang Sun, Jiqiang Wang, and Xinmin Chen. A review of hybrid-electric propulsion in aviation: Modeling methods, energy management strategies, and future prospects. *Aerospace*, 12(10):895, 2025.

[10] Jayant Mukhopadhaya and Brandon Graver. Performance analysis of regional electric aircraft. Technical report, International Council on Clean Transportation, July 2022.

[11] Giulio Avanzini, Emanuele L. de Angelis, and Fabrizio Giulietti. Optimal performance and sizing of a battery-powered aircraft. *Aerospace Science and Technology*, 59:132–144, 2016.

[12] Nicholas K. Borer, Michael D. Patterson, Jeffrey K. Viken, Clarke R. Moore, Joseph M. Phits, Benjamin J. Stoll, and Sean Clarke. Design of the x-57 maxwell prototyping aircraft. In *16th AIAA Aviation Technology, Integration, and Operations Conference*, 2016. AIAA Paper 2016-3154.

[13] David F. Finger, Carsten Braun, and Cees Bil. Comparison of hybrid-electric architectures for general aviation aircraft. *Journal of Aircraft*, 57(4):731–742, 2020.

[14] Mengyuan Wang, Suryanarayana Kolluri, Krishna A. Shah, Venkat R. Subramanian, and Mehran Mesbahi. Energy management for an all-electric aircraft via optimal control. *IEEE Transactions on Aerospace and Electronic Systems*, 59(2):1084–1095, 2023.

[15] Giuseppe Palaia, Karim Abu Salem, and Erasmo Carrera. Efficient methodology for power management optimization of hybrid-electric aircraft. *Aerospace*, 12(3):230, 2025.

[16] Reynard de Vries, Rob E. Wolleswinkel, Daniel Rosen Jacobsen, Maarten Bonnema, and Sebastian Thiede. Battery performance metrics for large electric passenger aircraft. In *Proceedings of the 34th Congress of the International Council of the Aeronautical Sciences*, Florence, Italy, 2024.

[17] Lukas Kiesewetter, Suryanarayana Kolluri, Mengyuan Wang, Ilias Belharouak, and Krishna A. Shah. Integrated analysis of electric aircraft performance and battery design through coupled modeling of flight and battery dynamics. *Journal of Power Sources*, 653:237679, 2025.

[18] Damien Lawhorn, Vandana Rallabandi, and Dan M. Ionel. Electric aircraft system co-simulation including body, propeller, propulsion, and energy storage models. In *2019 IEEE Transportation Electrification Conference and Expo (ITEC)*, pages 1–5, Novi, MI, USA, 2019.

[19] Felix Schweighofer, Benedikt Grüter, and Florian Holzapfel. Exploration of optimal control based surrogate modeling as a basis for fuel efficient 4d aircraft routing on graphs. *CEAS Aeronautical Journal*, 15:363–383, 2024.

[20] Enis T. Turgut, Mustafa Cavcar, Oznur Usanmaz, A. Ozan Canarslanlar, Tuncay Dogeroglu, Kadir Armutlu, and Ozan D. Yay. Fuel flow analysis for the cruise phase of commercial aircraft on domestic routes. *Aerospace Science and Technology*, 37:1–9, 2014.

[21] Priyank Pradeep and et al. Parametric study of state-of-charge for an electric aircraft in urban air mobility. In *AIAA Aviation 2021 Forum*, 2021. AIAA Paper 2021-3181.

[22] Kashif Mehmood and et al. Flight dynamic characteristics of wide-body aircraft with wind gust and turbulence. *Fluids*, 8(12):320, 2023.

[23] Z. Wu and Y. Cao. Gust loads on aircraft. *The Aeronautical Journal*, 123(1266):1216–1274, 2019.

[24] European Union Aviation Safety Agency. Easa certifies electric aircraft: First type certification for fully electric plane worldwide, June 2020. [Online]. Available: https://www.easa.europa.eu/en/newsroom-and-events/press-releases/easa-certifies-electric-aircraft-first-type-certification-fully (Accessed: 2026-06-15).

[25] Nicoletta Fala, Georgios Georgalis, and Nastaran Arzamani. Study on machine learning methods for general aviation flight phase identification. *Journal of Aerospace Information Systems*, 20(10):636–647, 2023.